# ANISOTROPIC POROUS PLASTICITY MODELS FOR DUCTILE FRACTURE

Ahmed Benallal, Ayrton Ferreira, Sergio Proença

# ANISOTROPIC POROUS PLASTICITY MODELS FOR DUCTILE FRACTURE

Ahmed Benallal *[1], Ayrton Ferreira[1,2], and Sergio Proença[2]
[1]*LMT, ENS Paris Saclay/CNRS/Université Paris Saclay*
[2]*Department of Structural Engineering, EESC, University of São Paulo, Brazil*

*Summary* General plastic models for ductile fracture are developed for voided materials with anisotropic matrix behaviour based on the concept of Isotropic Plastic Equivalent (IPE) space proposed by Karafillis and Boyce [1] and the general isotropic formulation provided in Benallal [2]. This allows all material symmetries to be included in a straightforward manner in the Gurson framework [3] to obtain anisotropic effective yield surfaces for porous materials. A numerical simulation is provided for illustration.

## MATRIX BEHVIOUR AND MICROSCOPIC DISSIPATION FUNCTION

The Gurson model [3] for porous materials is very effective and widely used in a lot of practical applications. Other important applications, among which metal forming for instance, need the inclusion of the anisotropy of the matrix stemming from its manufacturing process.

### Matrix behaviour

The anisotropic yield criterion for the matrix considered herein is based on the concept of an Isotropic Plasticity Equivalent (IPE) material as proposed by Karafillis and Boyce [1]. This concept consists in defining an auxiliary stress tensor $\boldsymbol{\sigma}^*$ in such a way that an actual anisotropic yield function $\phi^*(\boldsymbol{\sigma})$ can be equivalently obtained from an isotropic yield function $\phi(\boldsymbol{\sigma}^*)$ in terms of the auxiliary stress. Using a linear transformation of the stress state of the anisotropic material $\boldsymbol{\sigma}^* = \mathbb{L} : \boldsymbol{\sigma}$ yields therefore the general anisotropic yield function $\phi(\mathbb{L} : \boldsymbol{\sigma})$ for any isotropic yield function $\phi$. We consider here $\phi(\boldsymbol{\sigma}) = \sigma_{eq} g(\omega)$ where $\sigma_{eq} = \sqrt{(2/3)\mathbf{s} : \mathbf{s}}$ is the Von Mises effective stress , $\mathbf{s}$ the stress deviator and $\omega$ its Lode angle. Function $g$ is positive and chosen such that the yield function is convex. The yield domain is thus defined by $D^* = \{\boldsymbol{\sigma} | \phi(\mathbb{L} : \boldsymbol{\sigma}) \leq \sigma_0\}$, $\sigma_0$ being the yield stress.The fourth order tensor $\mathbb{L}$ used in the IPE stress transformation must exhibit the material internal symmetries and should also be traceless for isochoric plastic deformation. Note that only the first plastic yield is considered and evolution in anisotropy with further plastic strain is currently neglected.

### The maximum dissipation function

The maximum dissipation function that we denote $\pi(\dot{\boldsymbol{\epsilon}})$ is important in the derivation of the effective behaviour. It is the maximum of $\boldsymbol{\sigma} : \dot{\boldsymbol{\epsilon}}$over all stress states belonging to the closed yield domain $D^*$ or the support function of this domain. Using the procedure given in [2], one can show that for incompressible strain rates (considered here) this function reads

$$\pi(\dot{\boldsymbol{\epsilon}}) = \sigma_0 \frac{\dot{\epsilon}^*_{eq}}{\sqrt{g^2(\omega^*) + (g'(\omega^*))^2}} \tag{1}$$

where $\dot{\boldsymbol{\epsilon}}^* = \mathbb{L}^{T+} : \dot{\boldsymbol{\epsilon}}$, $\dot{\epsilon}^*_{eq}$ its effective component. Further, $\omega^*$ is the Lode angle of the auxiliary stress $\boldsymbol{\sigma}^*$ related to $\dot{\boldsymbol{\epsilon}}^*$ by the flow rule and given by the implicite relation $\zeta^* = \omega^* + \arctan \frac{g'(\omega^*)}{g(\omega^*)}$ with $\zeta^*$ the Lode angle of $\dot{\boldsymbol{\epsilon}}^*$. Finally, $\mathbb{L}^{T+}$ : is the Moore-Penrose inverse of the transpose of $\mathbb{L}$.

## EFFECTIVE YIELD SURFACE FOR ANISOTROPIC MATERIALS

The effective yield surface is obtained by exactly the same procedure as Gurson [3] coupling a homogenization scheme to the kinematic theorem of limit analysis using a hollow spherical cell $V$ with porosity $f$ and external radius $b$, the anisotropic rigid-plastic matrix behaviour depicted in the former section and the same incompressible kinematically admissible velocity trial field $\mathbf{v}(\mathbf{x}) = \dot{\mathbf{E}}' \cdot \mathbf{x} + (b^3/r^2)\dot{E}_m \mathbf{x}$ compatible with the prescribed macroscopic rate of deformation $\dot{\mathbf{E}}$ (with deviator $\dot{\mathbf{E}}'$ and volumetric part $\dot{E}_m$) at the boundary of the hollow sphere. This allows deriving upper bounds to the macroscopic stresses required to sustain plastic flow and these upper bound macroscopic stresses for the considered cell geometry and a for a range of macroscopic deformation rates allow to construct an upper bound yield locus for the porous material. These stresses are defined by the parametric form (the parameters being the macroscopic strain rate triaxaility and Lode angle plus the Euler angles defining the orientation of this strain rate with respect to material axes).

$$\boldsymbol{\Sigma} = \frac{\partial \Pi}{\partial \dot{\mathbf{E}}} \quad \text{with } \Pi(\dot{\mathbf{E}}) = \frac{1}{V} \int_V \pi(\dot{\boldsymbol{\epsilon}}(\dot{\mathbf{E}})) dV \tag{2}$$

$\Pi(\dot{\mathbf{E}})$ being the upper bound (to the exact macroscopic dissipation) obtained by the trial kinematically admissible velocity field and $\pi(\dot{\boldsymbol{\epsilon}})$ is the microscopic dissipation defined in the former section. One can show the existence of three functions $P$, $Q$ and $R$, all dependent on the macroscopic stress $\Sigma$ and the porosity $f$ such that the following semi-explicit form can represent the effective yield domain (the three functions are not obtained explicitely)

$$\frac{3}{2}\left(\frac{\mathbb{L} : \Sigma - P}{R}\right) : \left(\frac{\mathbb{L} : \Sigma - P}{R}\right) + 2f \cosh\left(\frac{3(\Sigma_m - Q)}{2R}\right) = 1 + f^2 \tag{3}$$

*Corresponding author. E-mail: benallal@ens-paris-saclay.fr

## ILLUSTRATION

The full procedure is illustrated here for the following data: the function $g$ defining the underlying isotropic yield function proposed in [1] is given by $g(\omega) = \frac{2}{3}\left\{\frac{1}{2}\left[(1-c)\varphi_1(\omega) + c\left(\frac{3^m}{2^{m-1}+1}\right)\varphi_2(\omega)\right]\right\}^{1/m}$ with $\varphi_1(\omega) = \left[\cos(\omega_1) - \cos(\omega_2)\right]^m + \left[\cos(\omega_2) - \cos(\omega_3)\right]^m + \left[\cos(\omega_3) - \cos(\omega_1)\right]^m$ and $\varphi_2(\omega) = \left[\cos(\omega_1)\right]^m + \left[\cos(\omega_2)\right]^m + \left[\cos(\omega_3)\right]^m$ while the linear transformations $\mathbb{L}$ representing material symmetries and used in the simulations are given in Table 1 with $\omega_1 = \omega$, $\omega_2 = \omega - 2\pi/3$ and $\omega_3 = \omega + 2\pi/3$.

Three examples are shown in Figure 1 for isotropic (I,left), transversaly isotropic (TI1,center) and orthotropic (O2,right) symmetries. The associated porosities and constitutive parameters ($m$, $c$) are provided in each of these figures while the anisotropy parameters are all gathered in Table 1. The figures show sections of the effective yield surfaces in the deviatoric principal plane at different mean stresses $\Sigma_m$. While for isotropic symmetry, the full yield surface can be represented in the principal stress space, one should emphasize that it is not the case for the two other symmetries. For the latter, only portions of the full yield surface can be represented there. The sections shown in these cases correspond to all loadings whose principal axes are aligned with the material axes and only to these loadings. All the simulations presented were performed suing numerical integration of the parametric relations (2).

$$\mathbb{L} = C\begin{bmatrix} L_{11} & L_{12} & L_{13} & 0 & 0 & 0 \\ L_{12} & L_{22} & L_{23} & 0 & 0 & 0 \\ L_{13} & L_{23} & L_{33} & 0 & 0 & 0 \\ 0 & 0 & 0 & 2L_{44} & 0 & 0 \\ 0 & 0 & 0 & 0 & 2L_{55} & 0 \\ 0 & 0 & 0 & 0 & 0 & 2L_{66} \end{bmatrix}$$

| Symm. | $L_{11}$ | $L_{22}$ | $L_{33}$ | $L_{44}$ | $L_{55}$ | $L_{66}$ |
|---|---|---|---|---|---|---|
| I | 1.0 | 1.0 | 1.0 | 0.75 | 0.75 | 0.75 |
| TI1 | 1.0 | 1.0 | 1.2 | 0.875 | 0.875 | 0.7 |
| O2 | 1.7 | 1.0 | 1.2 | 0.9 | 0.6 | 0.8 |

Table 1: The components $L_{ij}$ of the Voigt matricial representation of the linear transformation $\mathbb{L}$ and their values used in the simulation for the three different symmetries: Isotropic (I), Transverse isotropy (TI1) and orthotropy (O2). Note that due to incompressibility, we have $L_{12} = (L_{33} - L_{11} - L_{22})/2$, $L_{13} = (L_{22} - L_{33} - L_{11})/2$, $L_{23} = (L_{11} - L_{22} - L_{33})/2$

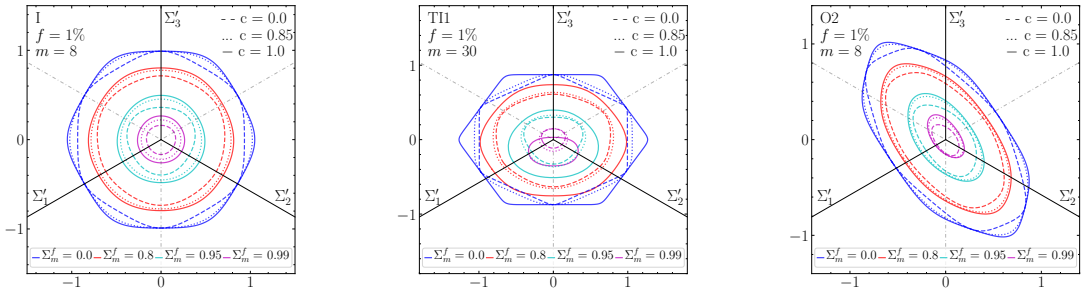


Figure 1: Sections of the effective yield surfaces in the deviatoric principal plane at different mean stresses $\Sigma_m$ for isotropy (left), transverse isotropy (center) and orthotropy (right) at porosity $f = .01$ and different $m$ and $c$ parameters. The scalar parameter $C$ is chosen for each case in such a way that the euclidean norm $||\mathbb{L}|| = \sqrt{5}$.

## CONCLUSIONS

A first step in developing anisotropic plastic porous models for ductile fracture has been achieved. These models need first to be compared to 3D numerical cell simulations to see how they perform and what are their limitations. Some efforts need to be put on the complete determination of the three functions $P$, $Q$ and $R$ in the same time as on the inclusion of other physical aspects of anisotropy such as morphological anisotropy and evolution of the anisotropy with ongoing plastic deformation.

## References

[1] Karafillis A. P. and Boyce M., A general anisotropic yield criterion using bounds and a transformation weighting tensor, *J. Mech. Phy. of Solids* **41**: 1859–1886, 1993.

[2] Benallal A., Constitutive equations for porous solids with matrix behaviour dependent on the second and third stress invariants, *Int. J. Impact Eng.*, **108**: 47–62, 2017.

[3] Gurson A. L.,Continuum theory of ductile rupture by void nucleation and growth: Part i–yield criteria and flow rules for porous ductile media, *J. Eng. Mat. and Tech.*, **99**: 2–15,1977.